Significant climate impacts of aerosol changes driven by growth in energy use and advances in emissions control technology

Alcide Zhao[1*], Massimo A. Bollasina[1], Monica Crippa[2] and David S. Stevenson[1]

[1] School of GeoSciences, University of Edinburgh, Edinburgh, UK

5   [2] European Commission, Joint Research Centre (JRC), Ispra, Italy

[*] Correspondence to: Alcide Zhao (alcide.zhao@ed.ac.uk)

Abstract. Anthropogenic aerosols have increased significantly since the industrial revolution, driven largely by growth in emissions from energy use in sectors including power generation, industry, and transport. Advances in emission control technologies since around 1970, however, have partially counteracted emissions increases from the above sectors. Using the

10   fully-coupled Community Earth System Model, we quantify the effective radiative forcing (ERF) and climate response to 1970-2010 aerosol emission changes associated with the above two policy-relevant emission drivers. Emissions from energy use growth generate a global mean aerosol ERF of -0.31 W m^{-2}, and result in a global mean cooling of -0.35 K and a precipitation reduction of -0.03 mm day^{-1}. By contrast, the avoided emissions from advances in emission control technology, which benefit air quality, generate a global mean ERF of +0.21 W m^{-2}, a global warming of +0.10 K and global mean

15   precipitation increase of +0.01 mm day^{-1}. The total net aerosol impacts on climate are dominated by energy use growth, from Asia in particular. However, technology advances outweigh energy use growth over Europe and North America. Also, the Arctic climate is significantly affected by aerosol emission changes from Europe, North America, and Asia. Various non-linear processes are involved along the pathway from aerosol emissions to radiative forcing and ultimately to climate responses, suggesting that the diagnosed aerosol forcing and effects must be interpreted in the context of experiment designs. Further, the

20   temperature response per unit aerosol ERF varies significantly across many factors, including location and magnitude of emission changes, implying that ERF, and the related metrics, need to be used very carefully for aerosols. Future aerosol emission pathways have large temporal and spatial uncertainties; our findings provide useful information for both assessing and interpreting such uncertainties, and may help inform future climate change impact reduction strategies.

1 Introduction

Climate change is driven by changes in a combination of natural and anthropogenic factors (Stocker et al., 2013). The increasing atmospheric abundance of greenhouse gases (GHGs) associated with human activities has long been recognized as the major driver of global warming since the industrial revolution. Additionally, anthropogenic emissions of aerosols and their

5 precursor gases have also led to significant climate impacts (Boucher et al., 2013), in addition to their detrimental effects on atmospheric visibility, human health and ecosystems. Aerosols can influence climate by absorbing/scattering shortwave radiation (aerosol-radiation interactions; Haywood and Ramaswamy (1998)), and by modifying cloud microphysics and precipitation processes (aerosol-cloud interactions; Fan et al. (2016)). Overall, aerosol emissions cause a net cooling of the Earth; almost a third of the warming from increases in GHGs is thought to have been counteracted by cooling due to increased

10 anthropogenic aerosols since the 1950s (Stocker et al., 2013). Yet, despite extensive research in the last decade that has led to significant progress in our understanding of the effects of aerosols (Ming and Ramaswamy, 2009; Shindell and Faluvegi, 2009; Allen and Sherwood, 2011; Bollasina et al., 2011; Ming and Ramaswamy, 2011; Ming et al., 2011; Boucher et al., 2013; Hwang et al., 2013; Wilcox et al., 2013; Xie et al., 2013; Shindell, 2014; Wang et al., 2015), there are still major uncertainties associated with their impacts on climate (Carslaw et al., 2013a; Fan et al., 2016; Lee et al., 2016; Fletcher et al., 2018).

15 In fact, aerosol forcing remains the dominant uncertainty in current estimates of radiative forcing on climate since pre-industrial times (Myhre et al., 2013). This is because of compounding uncertainties associated with the large spatial and temporal variability of aerosols, their short lifetimes, their diverse physical and chemical properties, and complex interactions with radiation and microphysical processes (Boucher et al., 2013; Carslaw et al., 2013b; Fan et al., 2016). For example, the sign and magnitude of the effect of aerosols on clouds and precipitation can vary substantially depending on emission locations,

20 forcing types as well as meteorological conditions (Rosenfeld et al., 2008; Stevens and Feingold, 2009; Yu et al., 2014; Malavelle et al., 2017; Kasoar et al., 2018). Also, there are large uncertainties due to the incomplete knowledge of both historical aerosol emissions and how they will evolve in the future (Gidden et al., 2018). All these uncertainties make it challenging to project future climate and to quantify the associated impacts on a range of sectors. More importantly, despite ongoing debates (Feichter et al., 2004; Xie et al., 2013; Wilcox et al., 2018), a large body of studies indicate that, per unit of

25 forcing/warming, aerosols have significantly larger impacts than GHGs on both global mean climate (Hansen et al., 2005; Shindell, 2014; Shindell et al., 2015), as well as global/regional climate extremes (Perkins, 2015; Xu et al., 2015; Lin et al., 2016; Wang et al., 2016; Samset et al., 2018a; Zhao et al., 2018; Zhao et al., 2019).

Emissions of anthropogenic aerosols have followed opposite trends between developed (decreases) and developing (increases) regions during the past few decades. For example, emissions of SO_2 from Asia increased steadily since the 1950s, while

30 emissions from Europe and North America started to decline after the 1970s (Smith et al., 2011; Wang et al., 2015; Crippa et al., 2016). The decline of air pollutant emissions in Europe and North America dates back to around 1970 when the first air quality directives were implemented at the continental scale (Crippa et al., 2016). By comparison, only after about 2010 have

some developing countries started to take mitigation measures. For example, Chinese SO_2 emissions have shown a noticeable decline since around 2012 (Silver et al., 2018; Zheng et al., 2018). As a result, India has recently overtaken China as the largest present-day emitter of SO_2 (Li et al., 2017). Anthropogenic aerosol emissions will be further significantly reduced worldwide during the 21st century (Markandya et al., 2018). Aerosol mitigation, however, may lead to adverse climate impacts, such as

5   the increased risk of climate extremes (Kloster et al., 2010; Samset et al., 2018a; Zhao et al., 2018; Zhao et al., 2019). A number of equally-plausible future emission pathways have been designed to seek a compromise between the impacts of air pollution on environment and climate following aerosol abatement in the near-, medium-, and long-term (Gidden et al., 2018). The uncertainty in the emission pathway alone represents a key limiting factor to a robust quantification and isolation of the overall aerosol impact on climate. Yet, possible differences in the climate response to varying aerosol emissions trajectories,

10   all the other forcings being the same, have been mostly overlooked so far (e.g., Sillmann et al. (2013); Pendergrass et al. (2015); Bartlett et al. (2016)).

Emission changes described above are primarily associated with three important and largely regulated sectors (industry, power generation and transportation), while the residual contribution to emissions from residential and agricultural sectors is relatively stationary in time (Crippa et al., 2016; Hoesly et al., 2018). Also, such changes originate primarily from two

15   competing emission drivers: economic growth and policy-driven emission controls (Crippa et al., 2016). The former is associated with energy use growth within the three sectors described above, while the latter includes both air pollution abatement measures and technology advances (hereinafter technology advances for short). To quantify the impacts of these factors, Crippa et al. (2016) developed the Emission Database for Global Atmospheric Research (EDGAR) retrospective air pollution emission scenarios for the period 1970-2010 (Sect. 2.1). Using a coupled composition-climate model and these

20   scenarios, Turnock et al. (2016) investigated the influence of past avoided aerosol emissions due to legislation and technology measures on European air quality, human health and climate.

Here we employ the fully-coupled Community Earth System Model (CESM1) to examine the impacts of aerosol emission changes associated with the above two major competing drivers (energy use growth and technology advances) at both global and regional scales. The aerosol scenarios used here represent the best estimates of past emissions. Therefore, compared to

25   idealized experiments where aerosol emissions/concentrations are scaled rather arbitrarily, the implications of this work can be more informative for future decision-making. The EDGAR scenarios, CESM1 model overview and experiment design, as well as analysis methods, are introduced in Section 2, Section 3 presents the results followed by a discussion in Section 4, and a summary in Section 5.

2. Aerosol emission scenarios and model experiments

2.1 The EDGAR retrospective air pollution scenarios

Based on the EDGAR4.3.1 best estimates for 1970 (REF1970; Table 1) and 2010 (REF2010), the EDGAR retrospective emission scenarios were designed to quantify the effectiveness of 1970-2010 changes in energy use and efficiency, technology progress and end-of-pipe emission reduction measures (Crippa et al., 2016). These retrospective scenarios focus on sectors including power generation, industry and road transport (the most regulated sectors), whereas emissions from all other sectors are the same as REF2010. The highest emission scenario (STAG_TECH) assumes no further improvements in technologies and abatement measures after 1970, but energy use and different fuel mix as REF2010. The second and lowest emission scenario (STAG_ENE) assumes stagnation of energy consumption since 1970, while fuel mix, energy efficiency, emission factors and abatements are the same as REF2010. Therefore, the difference between REF2010 and STAG_TECH represents the 2010-1970 emission reductions due to technology advances. Similarly, the difference between REF2010 and STAG_ENE represents the 2010-1970 emission increase due to energy use growth. Note carefully that the retrospective emission scenarios were deliberately designed to have emission changes from these two competing drivers to not add up to those of the total 1970-2010 changes, for the aim of quantifying the associated impacts from a what-if perspective. For example, what would be expected if we had not introduced any emission control technologies since the 1970s (Crippa et al., 2016).

2.2 Model and experiment design

We carry out time-slice simulations for the period 1970-2010 (Table 1) using the fully-coupled Community Earth System Model (CESM1; Hurrell et al. (2013)) at the nominal 1-degree resolution. The motivation of carrying out time-slice model simulation for this particular period has been justified in Zhao et al. (2019b). The atmosphere component of CESM1 is the Community Atmosphere Model 5 (CAM5) in which concentrations of CO_2 and CH_4 are prescribed with seasonal cycles and latitude-gradients (Conley et al., 2012). CAM5 includes a three-mode (Aitken, accumulation, and coarse) aerosol scheme (Modal Aerosol Mode 3). Several aerosol species (sulphate, organic carbon (OC), black carbon (BC), sea-salt, and dust) are simulated and their number concentrations and mass are prognostically calculated. Simple gas-phase chemistry is included for sulphate species: SO_2 is converted into SO_4 through both gas-phase OH oxidation and aqueous-phase oxidation by H_2O_2 and O_3 (Liu et al., 2015a; Liu et al., 2015b; Tilmes et al., 2015). BC is emitted into the accumulation mode and ages, which allows it to be coated with soluble species (e.g., SO_4) and to nucleate cloud droplets (Conley et al., 2012; Liu et al., 2012). Long-lived GHGs, natural aerosols and other reactive gases emissions/concentrations are obtained from (Lamarque et al., 2010) for 1970 and (Lamarque et al., 2011) for 2010. Ozone concentrations for 1970 and 2010 are from the Whole Atmosphere Community Climate Model (WACCM) simulations (Marsh et al., 2013). Anthropogenic aerosols and their precursor emissions are from the EDGAR retrospective scenarios (Sect. 2.1). The EDGAR emission sectors are remapped to conform to CAM5 emissions following (Lamarque et al., 2010).

Two baseline experiments are firstly carried out, where the model is initialized from one (ensemble member No 34) of the transient simulations in 1970 and 2010, respectively, from the CESM1 large ensemble project (LENS; Kay et al. (2015)). Also, we have a number of perturbation runs (Table 1). For each case, we have a paired set of simulations: one with sea surface temperature and sea ice fixed (hereinafter Fsst), and the other with a fully coupled ocean (Fcpd). All Fcpd simulations were

5   integrated into equilibrium (i.e., where the climate system equilibrates to imposed permutations but the deep ocean) after the initial perturbation, with repeated annual cycles of the forcings. For example, the baseline simulations were integrated into equilibrium under constant 1970 and 2010 forcings (denoted as B70 and B10). Note carefully that the length of each integration is different, and is deemed sufficient for analysis once the top-of-the-atmosphere radiation imbalance does not show significant trends any more (stabilizing at ~0.3 W m^{-2} in this work) during the last few decades of each run, following recent works

10   (Samset et al., 2016; Myhre et al., 2017; Samset et al., 2018b). We analyse the last 30 years of each equilibrium simulation and show differences between the baseline and perturbed simulations. Specifically, we denote 'best estimate' as the response to the best estimate of 1970-2010 total net anthropogenic aerosol-related emissions, 'energy use growth' as the response to emissions increases due to growth in energy use, and 'technology advances' as the response to avoided emissions from advances in emission control technology. The statistical significance of the difference between each two (baseline and

15   perturbed) sets of 30-yr model runs is estimated by the two-sided student t-test (p-value <0.05).

The paired Fsst simulation is under the same forcings as the corresponding Fcpd simulation, and are integrated for 40 years from the initial condition. The last 30-years of each Fsst simulation is used to diagnose the effective radiative forcing (ERF) at the top-of-the-atmosphere (top of the model in this case, ~3.6 hPa) following Forster et al. (2016). Additionally, we carried out similar Fsst simulations to diagnose the ERFs of the best estimate of 1970-2010 changes in the three major anthropogenic

20   aerosol species (BC, OC and sulphate). For example, we have a perturbation Fsst run in which only emissions of sulphate species are changed back to 1970 levels while all other forcings are the same as B10 to diagnose the ERF due to 1970-2010 sulphate aerosol changes.

3 Effective radiative forcing and climate responses

3.1 Effective radiative forcing

25   Figure 1 shows changes in aerosol burdens and the diagnosed ERF associated with the best estimate of 1970-2010 emissions of BC, OC and sulphate species. It can be seen that changes in the burdens of all aerosol species are statistically significant almost worldwide, while areas with statistically significant ERFs are rather confined. Aerosol burdens display opposite changes between Asia and industrialized regions of Europe and North America. For instance, the burden of SO$_4$ increases by 5.6 mg m^{-2} in Asia but decreases by -4.0 mg m^{-2} in Europe. BC emissions generate a global mean positive radiative forcing of

30   +0.06 W m^{-2}; the ERF spatial pattern is positively correlated to that of the emissions, resulting in peak values over Asia and Africa. In contrast to BC, OC emissions generate a global mean negative forcing of -0.04 W m^{-2}; note also the general spatial

anti-correlation between OC burdens and ERFs. The global mean ERF of sulphate aerosols is small in magnitude because of the partial cancellation between the positive forcing from sulphate aerosol reductions over Europe and North America and the marked negative forcing from sulphate aerosol increases over Asia (Fig. 1f). Yet, it can be seen that regional ERF values are dominated by sulphate. It is worth noticing that the individual ERF values of each aerosol species do not add up to that due to

5   the simultaneous changes in all these at the global scale (Fig. 2d). A further discussion on this is provided in Sect. 4.1.

The spatial patterns of the changes in the 550-nm Aerosol Optical Depth (AOD) are strongly correlated with those of aerosol burden (compare Fig. 1a-c to Fig. 2a). Therefore, instead of aerosol burdens, we turn to change in the total AOD of all aerosol species for the three scenario experiments where all aerosol species change simultaneously. The total net 1970-2010 AOD changes (Fig.2a), not surprisingly, display a sharp contrast between Asia (+0.034) and Europe (-0.022) and North America (-

10   0.003). This, as described above, is mainly driven by changes in sulphate species (Fig. 1c). The 1970-2010 aerosol-related emission changes produce a global mean ERF of -0.11 W m^{-2}, with marked regional values over Europe (+2.29 W m^{-2}), North America (+0.24 W m^{-2}) and Asia (-1.06 W m^{-2}; Fig.3b). Emissions from energy use growth lead AOD to increase almost worldwide (Fig.2b), resulting in a global mean ERF of -0.31 W m^{-2}, with the most noticeable negative forcing of -0.88 W m^{-2} over Asia followed by -0.51 W m^{-2} over North America (Fig. 3b). By contrast, the avoided emissions due to technology

15   advances lead AOD to decrease predominately over the Northern Hemisphere (Fig. 2c), and generate a global mean positive forcing of +0.21 W m^{-2} (Fig. 2f). The most noticeable changes are found over Europe (+1.16 W m^{-2}) and North America (+0.55 W m^{-2}).

3.2 Temperature responses

Figure 4 shows the spatial distribution and zonal mean profile of the surface air temperature responses. Also see Fig. 3c for

20   the regional mean values. In response to the 1970-2010 aerosol reductions over Europe and North America, there is widespread warming over both Europe (+0.83 K) and the Arctic (+0.26 K), as well as a weak temperature increase over North America. On the contrary, cooling is found over Asia (-0.03 K), the Indian Ocean and the central North Pacific Ocean. The cooling is very likely due to Asian aerosol emissions, contrasting the widespread warming elsewhere related to aerosol reductions over Europe and North America. The zonal mean temperature profile displays weak warming in the Southern Hemisphere, but

25   insignificant changes over the Northern Hemisphere tropics and mid-latitudes. However, the temperature response (warming) is noticeably amplified over polar regions (e.g., +0.7 K over the Arctic). The Arctic warming amplification, primarily due to local sea-ice albedo positive feedbacks (Kay et al., 2012; Najafi et al., 2015; Sand et al., 2015; Navarro et al., 2016; Dobricic et al., 2019), is likely to be associated with the positive forcing (Fig. 2d) from aerosol reductions over Europe and North America (Navarro et al., 2016).

30   Aerosol-related emissions from energy use growth result in a relatively homogenous cooling that is statistically significant almost worldwide (Fig. 4b), with a global mean cooling of -0.35 K. The cooling is enhanced over the Arctic (-0.92 K), very likely to be related to Asian emissions due to energy use growth, on top of the smaller contributions of the relatively smaller

changes in aerosol emissions over Europe and North America (Fig. 2b). The zonal mean temperature response displays significant cooling across all latitude bands, with peak values found at the North Pole (up to -1.5 K). The avoided aerosol-related emissions from technology advances (Fig. 2c) lead the globe to warm by +0.10 K, with the most pronounced responses over the Arctic (+0.22 K) and North America (+0.18 K). The zonal mean temperature response is only distinguishable from zero over the Northern Hemisphere mid-latitudes (~30°N) and the polar regions. It is worth pointing out the noticeable cooling pattern over Europe despite the large positive forcing (+1.16 W m^{-2}; Fig. 4f). The responses in sea level pressure and 850 hPa winds (not shown) suggest a large contribution to the European temperature response from the atmospheric circulation adjustments, resulting in anomalous cold advection from higher latitudes that offset the effects of local positive radiative forcing (Undorf et al., 2018).

As described above, despite the broad consistency between the patterns of aerosol ERF (Fig. 2) and temperature responses (Fig. 4), there are also notable dissimilarities. This is particularly true at regional scales such as over Asia, Africa and Europe. To further investigate this, we calculate the temperature response per unit aerosol ERF (temperature sensitivity) over various domain (Fig. 5). It can be seen that the relationship between ERF and temperature response is far from being linear even at the global scale and over latitudinal bands. Also, note the negative temperature sensitivity values, suggesting that forcing and temperature response can be of opposite signs for aerosols. For example, the global mean sensitivity is estimated to be +1.17 and +0.48 K (W m^{-2})$^{-1}$ for energy use growth and technology advances experiment, respectively, but -0.81 K (W m^{-2})$^{-1}$ for the best estimate case. Further, even considering positive temperature sensitivity values only, there are substantial variations between regions and emission scenarios. A representative example is Europe, with both the largest regional temperature sensitivity of 1.28 K (W m^{-2})$^{-1}$ in the energy use growth experiment, and the smallest value (0.02 K (W m^{-2})$^{-1}$) in the technology advances experiment. Note also the very large temperature sensitivity value over the Arctic (~ 2 K (W m^{-2})$^{-1}$) because of the strong sea-ice albedo positive feedbacks which act to enhance the temperature response to a given forcing.

3.3 Precipitation responses

Changes in precipitation show complex spatial patterns (Fig. 6) and much larger uncertainties (Fig. 3d) compared to temperature responses. Overall, the 1970-2010 aerosol-related emission changes result in a global drying trend (-0.01 mm day^{-1}), with the most pronounced changes over Asia (-0.13 mm day^{-1}) and adjoining oceans. By comparison, Europe gets wetter (+0.05 mm day^{-1}; Fig. 6a). Also, there is a southward shift of the rain belt over the tropical oceans, indicating a zonal–mean southward shift of the Inter-Tropical Convergence Zone (ITCZ; Fig. 6).

The globe, especially land areas, gets drier in response to aerosol emissions from energy use growth (Fig. 6b). The precipitation change in Asia (-0.11 mm day^{-1}) is close to that associated with the best estimate of 1970-2010 aerosol changes (-0.13 mm day^{-1}). This suggests that aerosol emissions from energy use growth exert the predominant control on precipitation reduction over Asia. The drying is also notable over Europe (-0.05 mm day^{-1}). Along with precipitation decreases at almost all latitude bands and the tropics in particular, zonal mean precipitation changes show a weak but further southward shift of the ITCZ,

leading to a weak precipitation increases over the Southern Hemisphere subtropics (10-30°S). On the contrary, technology advances lead precipitation to increase globally (+0.01 mm day^{-1}) and particularly in the Northern Hemisphere. Nevertheless, precipitation decrease can still be seen over Southeast Asia, East China, northern Europe and USA. Meanwhile, the zonal mean precipitation profile shows a marked northward shift of the ITCZ with notable precipitation reductions over the Southern

5   Hemisphere tropics.

Generally, in all the three aerosol perturbation experiments, precipitation changes with temperature at a rate of ~0.09 mm day^{-1} K^{-1}. This is slightly larger than the estimate (~28.6 mm yr^{-1} K^{-1}, i.e., ~0.08 mm day^{-1} K^{-1}) for the slow climate response component derived from the Precipitation Driver Response Model Intercomparison Project (PDRMIP; Samset et al. (2016)). Most of the global and regional mean responses follow to some extent the linear increase (compare Fig. 3c to 3d), yet Asia

10   and Europe deviate drastically from the linear relationship. This may suggest that regional precipitation responses are not simply linked to temperature through energy budget constraints, but also depend on other factors such as prevailing circulation patterns and remote teleconnections (Bollasina et al., 2014; Wilcox et al., 2018; Lewinschal et al., 2019). Overall, the above indicates the importance of changes in aerosol emissions in both global and regional precipitation changes. This is particularly true for Asia and Europe where represent the major sources of present-day aerosol emissions. In addition, aerosol changes are

15   shown to have important influences on the ITCZ that tends to shift toward the warmer hemisphere (Allen and Sherwood, 2011; Hwang et al., 2013; Acosta Navarro et al., 2017; Liu et al., 2018).

4. Discussion

4.1 Nonlinearities and the importance of background aerosol levels

Instead of linearly attributing the total aerosol emission changes into individual contributing factors, a "what-if" approach was

20   adopted to develop the EDGAR retrospective emission scenarios (Crippa et al., 2016). This design is useful to assess the effectiveness of major drivers of aerosol emissions and allows us to show explicitly the policy-choice driven impacts, while accounting for nonlinear interplays between individual drivers. However, this approach adds extra nonlinearities to the results presented here in that, as discussed throughout this work, aerosol emissions from energy use growth and technology advances do not add up to the total net 1970-2010 emission changes. This may suggest the existence of other factors taking effects, yet

25   it is difficult to attribute the residuals to such factors. Nevertheless, even when total emissions are linearly decomposed into individual contributing factors, it is reasonable to expect both the radiative forcing and climate responses to not linearly add up because of a variety of intertwined mechanisms. For example, the location-dependent lifetime of different aerosol species (Liu et al., 2012), and the forcing efficacies (Kasoar et al., 2016; Aamaas et al., 2017).

In Sect. 3.1, we diagnosed the ERF associated with changes in each individual aerosol species as the differences between the

30   baseline Fsst simulation (B10) and the ones where the targeted species (e.g., BC) are kept constant at their 1970 levels while the others are as prescribed in B10. We note that changes in the burdens and AOD of the three aerosol species are identical to

those in the experiment where all the three species change simultaneously (B10-B70). However, the ERF estimates do not

linearly add up to the total. In fact, the residual (0.14 W m^{-2}) is even larger in magnitude than the 1970-2010 total net aerosol

ERF (-0.11 W m^{-2}). This reflects partly the nonlinear effect associated with the mixing states of aerosol species as well as the

importance of background aerosol loadings. This is particularly important for BC whose effects depend also on the presence

5   of sulphate and organic aerosols (Ramana et al., 2010). More specifically, BC particles tend to be coated with other species

(e.g., sulphate, ammonium, and organic carbon) during ageing processes, thereby enhancing the absorption of BC and

amplifying their radiative forcing (Haywood and Ramaswamy, 1998; Kim et al., 2008; Chung et al., 2012; Wu et al., 2016).

That is, the radiative forcing of BC may change with the ratio of BC to soluble aerosol species. In our case, the ERF of BC is

diagnosed as the difference between the baseline experiment (B10) and that with BC held at the 1970 levels, leading the latter

10   experiment to have a smaller ratio of BC to SO$_4$ and therefore smaller ERF. As a consequence, the ERF estimate due to the

1970-2010 changes in BC emissions may be overestimated and may contribute to nonlinearities in the ERF of individual

species. Note that these nonlinearities can be further enhanced by processes related to aerosol-cloud interactions, which is

difficult to be quantified (Fan et al., 2016; Forster et al., 2016).

Overall, the above discussion illustrates the importance of background aerosol concentrations in estimating the radiative

15   forcing of aerosols. For example, diagnosing the ERF of BC the other way round, namely, keeping all other aerosol species at

1970 levels while changing BC to 2010 levels, would likely result in different ERF estimates. Therefore, it is important to

carefully bear in mind the method used when interpreting the ERF and climate responses associated with aerosol changes. For

example, the single forcing experiments in the Coupled Model Intercomparison Project (CMIP5) (Taylor et al., 2012), the

PDRMIP and other idealized aerosol perturbation experiments (Wang et al., 2015; Samset et al., 2016; Kasoar et al., 2018;

20   Liu et al., 2018; Persad and Caldeira, 2018), as well as the upcoming AerChemMIP (Collins et al., 2017) model experiments

all need to be interpreted in the context of their experiment designs.

4.2 Caveats on the use of effective radiative forcing for aerosols

The ERF is generally deemed to be a useful indicator of temperature changes (Shindell and Faluvegi, 2009; Myhre et al., 2013;

Shindell et al., 2015; Forster et al., 2016; Lewinschal et al., 2019). Based on ERF, many metrics have been proposed to facilitate

25   comparing the effectiveness of various forcing agents. Also, these metrics are appealing to quickly assess the climate outcomes

of possible future emission pathways, and may hence provide useful information to policy-makers (Aamaas et al., 2017;

Lewinschal et al., 2019). However, it is known that forcing and temperature response are not necessarily collocated, due to

many other climate processes and feedbacks such as the atmospheric and oceanic heat transport, and atmospheric circulation

adjustments (Boer and Yu, 2003; Shindell et al., 2010; Bellouin et al., 2016; Persad and Caldeira, 2018). Specifically, ERF

30   and the associated metrics may work for well-mixed forcing agents such as GHGs (Zhao et al., 2019b). However, they are

misleading and open to dangerous miss-interpretation when used for aerosols and some other short-lived climate forcers

(having a lifetime shorter than CO$_2$, notably aerosols and ozone, and their precursor gases).

We stress here again that temperature responses do not necessarily follow the ERF of aerosols. The range (0.02-2 (W m^{-2})$^{-1}$) of the global mean temperature response per unit ERF is even larger than that (0.1-1.4 (W m^{-2})$^{-1}$) reported by Persad and Caldeira (2018). Also, our results suggest that the model simulated temperature response per unit aerosol ERF can differ considerably with even subtle differences in experiment design (e.g. with different amount of aerosols emitted in different

5   locations at different timings). Further, due to the fact that aerosol schemes are represented differently across present generation climate models; it is highly likely that the sensitivities will differ further upon the choice of climate models. Therefore, as also pointed out by recent works (Persad and Caldeira, 2018; Lewinschal et al., 2019), the large divergence in the temperature response per unit ERF from aerosols highlights the need to use ERF and derivative metrics carefully for aerosols.

4.3 Implications for future climate projection

10   Reliable projections of future climate under different but equally plausible emission pathways are of utmost importance to better constrain the range of possible societal risks and response options. Unfortunately, there are still considerable challenges due to limitations and uncertainties in our understanding of many aspects of the earth system (Knutti and Sedláček, 2013; Northrop and Chandler, 2014; Marotzke, 2019). Aerosols represent one of the largest sources of uncertainty (Boucher et al., 2013; Lee et al., 2016; Fletcher et al., 2018). Present-day anthropogenic aerosol emissions are largely influenced by sectors

15   including power generation, industry and transport. However, in some of the future emission pathways, for example the Tier-1 Shared Socioeconomic Pathways scenarios (SSP1; Gidden et al. (2018)), aerosol emissions are expected to decline drastically worldwide as we transit to non-fossil-fuel-based fields together with rapid implementation of air pollution control measures and new technologies. However, the timing and rate of such transitions are largely uncertain. On the other hand, it is also likely that aerosol emissions will increase, especially over some developing regions, under scenarios where high inequality exist

20   between and within countries. For example, in SSP3, expanding industrial sectors over Southeast Asia will rely continually on traditional energy sources such as coal. As a consequence, aerosol emissions from energy use are expected to increase and therefore offset aerosol reductions elsewhere.

The above reflects the large uncertainties (both spatially and temporally) in our understanding and estimates of future aerosol emission trajectories, given the possibility that very different future emission pathways may be adopted by different countries

25   to compromise between climate/air pollution impacts and economic growth. The large impacts of present-day aerosol emissions from the two competing drivers, as reported in this work, therefore suggest that the major drivers (e.g., future energy structure and efficiency, air pollution control measurements, as well as technology progresses) of aerosol emission changes may play even more important but uncertain roles in future climate projections. Nevertheless, our findings may help better assess and interpret such uncertainties in future climate projections.

5. Summary and conclusions

Using CESM1, time-slice simulations were carried out to investigate the ERF and climate impacts of 1970-2010 aerosol emission changes, focusing on two major policy-relevant emission drivers that compete: energy use growth and advances in emission control technology. The 1970-2010 anthropogenic aerosol emission changes generate an ERF of -0.11 W m^{-2}. This

5   is dominated by sulphate species, but the ERF estimates resolved into each individual species do not add up linearly to the total. The residual may be associated with the mixing states of different aerosol species (Kim et al., 2008), as well as many other intertwined nonlinear processes linking aerosol emissions to radiative forcing, and to temperature and precipitation responses. These nonlinearities highlight the importance that one must bear aerosol experiment designs carefully in mind when interpreting aerosol forcing and effects. Particularly, the background concentration of both GHGs and aerosols may have strong

10   influences on isolated aerosol effects using climate models (Regayre et al., 2018; Grandey and Wang, 2019).

Despite the global mean negative forcing from 1970-2010 aerosol changes, the global mean temperature increased by +0.09 K, while precipitation decreased by -0.01 mm day^{-1}. Energy use growth leads aerosols to increase over the Northern Hemisphere and Asia in particular, giving a global mean ERF of -0.31 W m^{-2}, and resulting in a homogenous global cooling (-0.41 K) and drying (-0.03 mm day^{-1}). On the contrary, the avoided aerosol emissions due to technology advances generate a

15   global mean ERF of +0.21 W m^{-2}, and result in global warming (+0.10 K) and wettening (+0.01 mm day^{-1}). Change in aerosol emissions and the resultant climate impacts are dominated by energy use growth over Asia but by technology advances over Europe and North America, while the global changes are a competition of these two drivers. Compared to the rest of the world, temperature responses in the Arctic are noticeably amplified because of positive feedback processes (Navarro et al., 2016; Wobus et al., 2016; Dobricic et al., 2019). The large temperature responses are likely to be related to changes in aerosol

20   emissions over Europe and North America, while our results demonstrate that aerosol emissions from Asia may also play an important role (Westervelt et al., 2015; Wang et al., 2018; Dobricic et al., 2019). The caveat is that all findings here may be model dependent, which is particularly the case for aerosols, given the high degree of parameterisation and divergence in aerosol schemes across present generation climate models. These findings, therefore, need to be verified using other models, while identifying the possible differences and reasons behind.

25   In conclusion, energy use growth and technology advances represent two major drivers of present-day aerosol emission changes, and have strong and competing impacts on present-day climate. We anticipate that there will be significant but uncertain changes in aerosol emissions over the coming decades driven by these two drivers. Also, there are a variety of nonlinearities in the effects of aerosols, originating from many factors including aerosol experiment design. All these uncertainties and nonlinearities may translate into even larger uncertainties in future climate projections and associated

30   impacts. Given all the findings and implications laid out above, we strongly encourage model groups to better constrain the nonlinearities and uncertainness associated with aerosols in their climate models. Also, we encourage the wider research

community to verify and further develop our findings in terms of aerosol-climate interactions and projections, as well as policy-

relevant aerosol emission changes and their influences on air quality and associated socioeconomic impacts.

Code and data availability: This work uses the Community Earth System Model on the ARCHER UK National Supercomputing Service. The model outputs were pre-processed using netCDF Operator (NCO) and Climate Data Operator (CDO). The analysis is carried out using the Python programming language. Data presented here can be freely accessed (embargoed) through the Edinburgh DataShare (https://datashare.is.ed.ac.uk/handle/10283/3369).

5 **Author contributions:** D.S. conceptualized the project. M.C. provided the EDGAR emission scenarios. A.Z. M.B. and D.S. planned and designed the experiments. A.Z. carried out all model experiments, analysed the model outputs and produced all results. The manuscript was drafted by A.Z., and improved with inputs from all other co-authors.

Competing interests: The authors declare no conflict of interest.

Acknowledgements: D. S. Stevenson acknowledges support from the NERC grant NE/N003411/1 and NE/S009019/1. M. A.

10 Bollasina was supported by the UK-China Research and Innovation Partnership Fund through the Met Office Climate Science for Service Partnership (CSSP) China as part of the Newton Fund (grant no. H5438500). This work used the ARCHER UK National Supercomputing Service (http://www.archer.ac.uk). The authors thank the Community Earth System Model project at NCAR. We are grateful to Gary Strand (NCAR) for providing the model dumps.

References

15 Aamaas, B., Berntsen, T. K., Fuglestvedt, J. S., Shine, K. P., and Collins, W. J.: Regional temperature change potentials for short-lived climate forcers based on radiative forcing from multiple models, Atmospheric Chemistry and Physics, 17, 10795-10809, 2017.
Acosta Navarro, J. C., Ekman, A. M., Pausata, F. S., Lewinschal, A., Varma, V., Seland, Ø., Gauss, M., Iversen, T., Kirkevåg, A., and Riipinen, I.: Future response of temperature and precipitation to reduced aerosol emissions as compared
20 with increased greenhouse gas concentrations, Journal of Climate, 30, 939-954, 2017.
Allen, R. J., and Sherwood, S. C.: The impact of natural versus anthropogenic aerosols on atmospheric circulation in the Community Atmosphere Model, Climate dynamics, 36, 1959-1978, 2011.
Bartlett, Bollasina, M. A., Booth, B. B., Dunstone, N. J., Marenco, F., Messori, G., and Bernie, D. J.: Do differences in future sulfate emission pathways matter for near-term climate? A case study for the Asian monsoon, AGU Fall Meeting
25 Abstracts, 2016,
Bellouin, N., Baker, L., Hodnebrog, Ø., Olivie, D., Cherian, R., Macintosh, C., Samset, B., Esteve, A., Aamaas, B., and Quaas, J.: Regional and seasonal radiative forcing by perturbations to aerosol and ozone precursor emissions, Atmospheric Chemistry and Physics, 16, 13885-13910, 2016.
Boer, G., and Yu, B.: Climate sensitivity and response, Climate Dynamics, 20, 415-429, 2003.
30 Bollasina, M. A., Ming, Y., and Ramaswamy, V.: Anthropogenic aerosols and the weakening of the South Asian summer monsoon, science, 334, 502-505, 2011.
Bollasina, M. A., Ming, Y., Ramaswamy, V., Schwarzkopf, M. D., and Naik, V.: Contribution of local and remote anthropogenic aerosols to the twentieth century weakening of the South Asian Monsoon, Geophysical Research Letters, 41, 680-687, 2014.
35 Boucher, O., Randall, D., Artaxo, P., Bretherton, C., Feingold, G., Forster, P., Kerminen, V.-M., Kondo, Y., Liao, H., and Lohmann, U.: Clouds and aerosols, in: Climate change 2013: the physical science basis. Contribution of Working Group I to the Fifth Assessment Report of the Intergovernmental Panel on Climate Change, Cambridge University Press, 571-657, 2013.
Carslaw, K., Lee, L., Reddington, C., Pringle, K., Rap, A., Forster, P., Mann, G., Spracklen, D., Woodhouse, M., and
40 Regayre, L.: Large contribution of natural aerosols to uncertainty in indirect forcing, Nature, 503, 67, 2013a.
Carslaw, K. S., Lee, L. A., Reddington, C. L., Mann, G. W., and Pringle, K. J.: The magnitude and sources of uncertainty in global aerosol, Faraday discussions, 165, 495-512, 2013b.
Chung, C., Lee, K., and Mueller, D.: Effect of internal mixture on black carbon radiative forcing, Tellus B: Chemical and Physical Meteorology, 64, 10925, 2012.
45 Collins, W. J., Lamarque, J.-F., Schulz, M., Boucher, O., Eyring, V., Hegglin, M. I., Maycock, A., Myhre, G., Prather, M., and Shindell, D.: AerChemMIP: quantifying the effects of chemistry and aerosols in CMIP6, Geoscientific Model Development, 10, 585-607, 2017.

Conley, A. J., Garcia, R., Kinnison, D., Lamarque, J.-F., Marsh, D., Mills, M., Smith, A. K., Tilmes, S., Vitt, F., and Morrison, H.: Description of the NCAR community atmosphere model (CAM 5.0), NCAR technical note, 2012.

Crippa, M., Janssens-Maenhout, G., Dentener, F., Guizzardi, D., Sindelarova, K., Muntean, M., Van Dingenen, R., and Granier, C.: Forty years of improvements in European air quality: regional policy-industry interactions with global impacts, Atmospheric Chemistry and Physics, 16, 3825-3841, 2016.

Dobricic, S., Pozzoli, L., Vignati, E., Van Dingenen, R., Wilson, J., Russo, S., and Klimont, Z.: Nonlinear impacts of future anthropogenic aerosol emissions on Arctic warming, Environmental Research Letters, 14, 034009, 2019.

Fan, J., Wang, Y., Rosenfeld, D., and Liu, X.: Review of aerosol–cloud interactions: Mechanisms, significance, and challenges, Journal of the Atmospheric Sciences, 73, 4221-4252, 2016.

Feichter, J., Roeckner, E., Lohmann, U., and Liepert, B.: Nonlinear aspects of the climate response to greenhouse gas and aerosol forcing, Journal of climate, 17, 2384-2398, 2004.

Fletcher, C. G., Kravitz, B., and Badawy, B.: Quantifying uncertainty from aerosol and atmospheric parameters and their impact on climate sensitivity, Atmospheric Chemistry and Physics, 18, 17529-17543, 2018.

Forster, P. M., Richardson, T., Maycock, A. C., Smith, C. J., Samset, B. H., Myhre, G., Andrews, T., Pincus, R., and Schulz, M.: Recommendations for diagnosing effective radiative forcing from climate models for CMIP6, Journal of Geophysical Research: Atmospheres, 121, 2016.

Gidden, M., Riahi, K., Smith, S., Fujimori, S., Luderer, G., Kriegler, E., van Vuuren, D. P., van den Berg, M., Feng, L., and Klein, D.: Global emissions pathways under different socioeconomic scenarios for use in CMIP6: a dataset of harmonized emissions trajectories through the end of the century, Geoscientific Model Development Discussions, 1-42, 2018.

Grandey, B. S., and Wang, C.: Background Conditions Influence the Estimated Cloud Radiative Effects of Anthropogenic Aerosol Emissions From Different Source Regions, Journal of Geophysical Research: Atmospheres, 124, 2276-2295, 2019.

Hansen, J., Sato, M., Ruedy, R., Nazarenko, L., Lacis, A., Schmidt, G., Russell, G., Aleinov, I., Bauer, M., and Bauer, S.: Efficacy of climate forcings, Journal of Geophysical Research: Atmospheres, 110, 2005.

Haywood, J., and Ramaswamy, V.: Global sensitivity studies of the direct radiative forcing due to anthropogenic sulfate and black carbon aerosols, Journal of Geophysical Research: Atmospheres, 103, 6043-6058, 1998.

Hoesly, R. M., Smith, S. J., Feng, L., Klimont, Z., Janssens-Maenhout, G., Pitkanen, T., Seibert, J. J., Vu, L., Andres, R. J., and Bolt, R. M.: Historical (1750–2014) anthropogenic emissions of reactive gases and aerosols from the Community Emissions Data System (CEDS), Geoscientific Model Development, 11, 369-408, 2018.

Hurrell, J. W., Holland, M. M., Gent, P. R., Ghan, S., Kay, J. E., Kushner, P. J., Lamarque, J.-F., Large, W. G., Lawrence, D., and Lindsay, K.: The community earth system model: a framework for collaborative research, Bulletin of the American Meteorological Society, 94, 1339-1360, 2013.

Hwang, Y. T., Frierson, D. M., and Kang, S. M.: Anthropogenic sulfate aerosol and the southward shift of tropical precipitation in the late 20th century, Geophysical Research Letters, 40, 2845-2850, 2013.

Kasoar, M., Voulgarakis, A., Lamarque, J.-F., Shindell, D. T., Bellouin, N., Collins, W. J., Faluvegi, G., and Tsigaridis, K.: Regional and global temperature response to anthropogenic SO 2 emissions from China in three climate models, Atmospheric Chemistry and Physics, 16, 9785-9804, 2016.

Kasoar, M., Shawki, D., and Voulgarakis, A.: Similar spatial patterns of global climate response to aerosols from different regions, npj Climate and Atmospheric Science, 1, 12, 2018.

Kay, J., Deser, C., Phillips, A., Mai, A., Hannay, C., Strand, G., Arblaster, J., Bates, S., Danabasoglu, G., and Edwards, J.: The Community Earth System Model (CESM) large ensemble project: A community resource for studying climate change in the presence of internal climate variability, Bulletin of the American Meteorological Society, 96, 1333-1349, 2015.

Kay, J. E., Holland, M. M., Bitz, C. M., Blanchard-Wrigglesworth, E., Gettelman, A., Conley, A., and Bailey, D.: The influence of local feedbacks and northward heat transport on the equilibrium Arctic climate response to increased greenhouse gas forcing, Journal of Climate, 25, 5433-5450, 2012.

Kim, D., Wang, C., Ekman, A. M., Barth, M. C., and Rasch, P. J.: Distribution and direct radiative forcing of carbonaceous and sulfate aerosols in an interactive size-resolving aerosol–climate model, Journal of geophysical research: Atmospheres, 113, 2008.

Kloster, S., Dentener, F., Feichter, J., Raes, F., Lohmann, U., Roeckner, E., and Fischer-Bruns, I.: A GCM study of future climate response to aerosol pollution reductions, Climate dynamics, 34, 1177-1194, 2010.

Knutti, R., and Sedláček, J.: Robustness and uncertainties in the new CMIP5 climate model projections, Nature Climate Change, 3, 369, 2013.

Lamarque, J.-F., Bond, T. C., Eyring, V., Granier, C., Heil, A., Klimont, Z., Lee, D., Liousse, C., Mieville, A., and Owen, B.: Historical (1850–2000) gridded anthropogenic and biomass burning emissions of reactive gases and aerosols: methodology and application, Atmospheric Chemistry and Physics, 10, 7017-7039, 2010.

Lamarque, J.-F., Kyle, G. P., Meinshausen, M., Riahi, K., Smith, S. J., van Vuuren, D. P., Conley, A. J., and Vitt, F.: Global and regional evolution of short-lived radiatively-active gases and aerosols in the Representative Concentration Pathways, Climatic change, 109, 191-212, 2011.

Lee, L. A., Reddington, C. L., and Carslaw, K. S.: On the relationship between aerosol model uncertainty and radiative forcing uncertainty, Proceedings of the National Academy of Sciences, 113, 5820-5827, 2016.

Lewinschal, A., Ekman, A. M., Hansson, H.-C., Sand, M., Berntsen, T. K., and Langner, J.: Local and remote temperature response of regional SO 2 emissions, Atmospheric Chemistry and Physics, 19, 2385-2403, 2019.

Li, McLinden, C., Fioletov, V., Krotkov, N., Carn, S., Joiner, J., Streets, D., He, H., Ren, X., and Li, Z.: India is overtaking China as the world's largest emitter of anthropogenic sulfur dioxide, Scientific reports, 7, 14304, 2017.

Lin, L., Wang, Z., Xu, Y., and Fu, Q.: Sensitivity of precipitation extremes to radiative forcing of greenhouse gases and aerosols, Geophysical Research Letters, 43, 9860-9868, 2016.

Liu, L., Shawki, D., Voulgarakis, A., Kasoar, M., Samset, B., Myhre, G., Forster, P., Hodnebrog, Ø., Sillmann, J., and Aalbergsjø, S.: A PDRMIP Multimodel Study on the impacts of regional aerosol forcings on global and regional precipitation, Journal of Climate, 31, 4429-4447, 2018.

Liu, S., Aiken, A. C., Gorkowski, K., Dubey, M. K., Cappa, C. D., Williams, L. R., Herndon, S. C., Massoli, P., Fortner, E. C., and Chhabra, P. S.: Enhanced light absorption by mixed source black and brown carbon particles in UK winter, Nature communications, 6, 8435, 2015a.

Liu, X., Easter, R. C., Ghan, S. J., Zaveri, R., Rasch, P., Shi, X., Lamarque, J.-F., Gettelman, A., Morrison, H., and Vitt, F.: Toward a minimal representation of aerosols in climate models: Description and evaluation in the Community Atmosphere Model CAM5, Geoscientific Model Development, 5, 709, 2012.

Liu, X., Ma, P.-L., Wang, H., Tilmes, S., Singh, B., Easter, R., Ghan, S., and Rasch, P.: Description and evaluation of a new 4-mode version of Modal Aerosol Module (MAM4) within version 5.3 of the Community Atmosphere Model, Geoscientific Model Development Discussions, 8, 2015b.

Malavelle, F. F., Haywood, J. M., Jones, A., Gettelman, A., Clarisse, L., Bauduin, S., Allan, R. P., Karset, I. H. H., Kristjánsson, J. E., and Oreopoulos, L.: Strong constraints on aerosol–cloud interactions from volcanic eruptions, Nature, 546, 485, 2017.

Markandya, A., Sampedro, J., Smith, S. J., Van Dingenen, R., Pizarro-Irizar, C., Arto, I., and González-Eguino, M.: Health co-benefits from air pollution and mitigation costs of the Paris Agreement: a modelling study, The Lancet Planetary Health, 2, e126-e133, 2018.

Marotzke, J.: Quantifying the irreducible uncertainty in near-term climate projections, Wiley Interdisciplinary Reviews: Climate Change, 10, e563, 2019.

Marsh, D. R., Mills, M. J., Kinnison, D. E., Lamarque, J.-F., Calvo, N., and Polvani, L. M.: Climate change from 1850 to 2005 simulated in CESM1 (WACCM), Journal of climate, 26, 7372-7391, 2013.

Ming, Y., and Ramaswamy, V.: Nonlinear climate and hydrological responses to aerosol effects, Journal of Climate, 22, 1329-1339, 2009.

Ming, Y., and Ramaswamy, V.: A model investigation of aerosol-induced changes in tropical circulation, Journal of Climate, 24, 5125-5133, 2011.

Ming, Y., Ramaswamy, V., and Chen, G.: A model investigation of aerosol-induced changes in boreal winter extratropical circulation, Journal of Climate, 24, 6077-6091, 2011.

Myhre, Forster, P., Samset, B., Hodnebrog, Ø., Sillmann, J., Aalbergsjø, S., Andrews, T., Boucher, O., Faluvegi, G., and Fläschner, D.: PDRMIP: A precipitation driver and response model intercomparison project—Protocol and preliminary results, Bulletin of the American Meteorological Society, 98, 1185-1198, 2017.

Myhre, G., Shindell, D., Bréon, F.-M., Collins, W., Fuglestvedt, J., Huang, J., Koch, D., Lamarque, J.-F., Lee, D., and Mendoza, B.: Anthropogenic and natural radiative forcing, Climate change, 423, 2013.

Najafi, M. R., Zwiers, F. W., and Gillett, N. P.: Attribution of Arctic temperature change to greenhouse-gas and aerosol influences, Nature Climate Change, 5, 246-249, 2015.

Navarro, J. A., Varma, V., Riipinen, I., Seland, Ø., Kirkevåg, A., Struthers, H., Iversen, T., Hansson, H.-C., and Ekman, A.: Amplification of Arctic warming by past air pollution reductions in Europe, Nature Geoscience, 2016.

Northrop, P. J., and Chandler, R. E.: Quantifying sources of uncertainty in projections of future climate, Journal of Climate, 27, 8793-8808, 2014.

Pendergrass, A. G., Lehner, F., Sanderson, B. M., and Xu, Y.: Does extreme precipitation intensity depend on the emissions scenario?, Geophysical Research Letters, 42, 8767-8774, 2015.

Perkins, S. E.: A review on the scientific understanding of heatwaves—their measurement, driving mechanisms, and changes at the global scale, Atmospheric Research, 164, 242-267, 2015.

Persad, G. G., and Caldeira, K.: Divergent global-scale temperature effects from identical aerosols emitted in different regions, Nature communications, 9, 3289, 2018.

Ramana, M., Ramanathan, V., Feng, Y., Yoon, S., Kim, S., Carmichael, G., and Schauer, J.: Warming influenced by the ratio of black carbon to sulphate and the black-carbon source, Nature Geoscience, 3, 542, 2010.

Regayre, L. A., Johnson, J. S., Yoshioka, M., Pringle, K. J., Sexton, D. M., Booth, B. B., Lee, L. A., Bellouin, N., and Carslaw, K. S.: Aerosol and physical atmosphere model parameters are both important sources of uncertainty in aerosol ERF, Atmospheric Chemistry and Physics, 18, 9975-10006, 2018.

Rosenfeld, D., Lohmann, U., Raga, G. B., O'Dowd, C. D., Kulmala, M., Fuzzi, S., Reissell, A., and Andreae, M. O.: Flood or drought: how do aerosols affect precipitation?, science, 321, 1309-1313, 2008.

Samset, B., Myhre, G., Forster, P., Hodnebrog, Ø., Andrews, T., Faluvegi, G., Flaeschner, D., Kasoar, M., Kharin, V., and Kirkevåg, A.: Fast and slow precipitation responses to individual climate forcers: A PDRMIP multimodel study, Geophysical Research Letters, 43, 2782-2791, 2016.

Samset, B., Sand, M., Smith, C., Bauer, S., Forster, P., Fuglestvedt, J., Osprey, S., and Schleussner, C. F.: Climate impacts from a removal of anthropogenic aerosol emissions, Geophysical Research Letters, 45, 1020-1029, 2018a.

Samset, B., Sand, M., Smith, C., Bauer, S., Forster, P., Fuglestvedt, J., Osprey, S., and Schleussner, C. F.: Climate impacts from a removal of anthropogenic aerosol emissions, Geophysical Research Letters, 2018b.

Sand, M., Berntsen, T., von Salzen, K., Flanner, M., Langner, J., and Victor, D.: Response of Arctic temperature to changes in emissions of short-lived climate forcers, Nature Climate Change, 2015.

Shindell: Inhomogeneous forcing and transient climate sensitivity, Nature Climate Change, 4, 274, 2014.

Shindell, Faluvegi, G., Rotstayn, L., and Milly, G.: Spatial patterns of radiative forcing and surface temperature response, Journal of Geophysical Research: Atmospheres, 120, 5385-5403, 2015.

Shindell, D., and Faluvegi, G.: Climate response to regional radiative forcing during the twentieth century, Nature Geoscience, 2, 294, 2009.

Shindell, D., Schulz, M., Ming, Y., Takemura, T., Faluvegi, G., and Ramaswamy, V.: Spatial scales of climate response to inhomogeneous radiative forcing, Journal of Geophysical Research: Atmospheres, 115, 2010.

Sillmann, J., Pozzoli, L., Vignati, E., Kloster, S., and Feichter, J.: Aerosol effect on climate extremes in Europe under different future scenarios, Geophysical Research Letters, 40, 2290-2295, 2013.

Silver, B., Reddington, C., Arnold, S., and Spracklen, D.: Substantial changes in air pollution across China during 2015–2017, Environmental Research Letters, 13, 114012, 2018.

Smith, S. J., Aardenne, J. v., Klimont, Z., Andres, R. J., Volke, A., and Delgado Arias, S.: Anthropogenic sulfur dioxide emissions: 1850–2005, Atmospheric Chemistry and Physics, 11, 1101-1116, 2011.

Stevens, B., and Feingold, G.: Untangling aerosol effects on clouds and precipitation in a buffered system, Nature, 461, 607, 2009.

Stocker, Qin, D., Plattner, G.-K., Tignor, M., Allen, S. K., Boschung, J., Nauels, A., Xia, Y., Bex, V., and Midgley, P. M.: Climate change 2013: The physical science basis, Intergovernmental Panel on Climate Change, Working Group I Contribution to the IPCC Fifth Assessment Report (AR5)(Cambridge Univ Press, New York), 2013.

Taylor, K. E., Stouffer, R. J., and Meehl, G. A.: An overview of CMIP5 and the experiment design, Bulletin of the American Meteorological Society, 93, 485-498, 2012.

Tilmes, S., Lamarque, J.-F., Emmons, L., Kinnison, D., Ma, P., Liu, X., Ghan, S., Bardeen, C., Arnold, S., and Deeter, M.: Description and evaluation of tropospheric chemistry and aerosols in the Community Earth System Model (CESM1. 2), Geoscientific Model Development, 8, 1395-1426, 2015.

Turnock, S., Butt, E., Richardson, T., Mann, G., Reddington, C., Forster, P., Haywood, J., Crippa, M., Janssens-Maenhout, G., and Johnson, C.: The impact of European legislative and technology measures to reduce air pollutants on air quality, human health and climate, Environmental Research Letters, 11, 024010, 2016.

Undorf, S., Bollasina, M., Booth, B., and Hegerl, G.: Contrasting the Effects of the 1850–1975 Increase in Sulphate Aerosols from North America and Europe on the Atlantic in the CESM, Geophysical Research Letters, 45, 11,930-911,940, 2018.

Wang, Lin, L., Yang, M., and Xu, Y.: The effect of future reduction in aerosol emissions on climate extremes in China, Climate Dynamics, 1-15, 2016.

Wang, Jiang, J. H., Su, H., Choi, Y.-S., Huang, L., Guo, J., and Yung, Y. L.: Elucidating the role of anthropogenic aerosols in Arctic sea ice variations, Journal of Climate, 31, 99-114, 2018.

Wang, Y., Jiang, J. H., and Su, H.: Atmospheric responses to the redistribution of anthropogenic aerosols, Journal of Geophysical Research: Atmospheres, 120, 9625-9641, 2015.

Westervelt, D., Horowitz, L., Naik, V., Golaz, J.-C., and Mauzerall, D.: Radiative forcing and climate response to projected 21st century aerosol decreases, Atmospheric Chemistry and Physics, 15, 12681-12703, 2015.

Wilcox, L., Dunstone, N., Lewinschal, A., Bollasina, M., Ekman, A., and Highwood, E.: Mechanisms for a remote response to Asian aerosol emissions in boreal winter, Atmospheric Chemistry and Physics Discussions, 2018.

Wilcox, L. J., Highwood, E. J., and Dunstone, N. J.: The influence of anthropogenic aerosol on multi-decadal variations of historical global climate, Environmental Research Letters, 8, 024033, 2013.

Wobus, C., Flanner, M., Sarofim, M. C., Moura, M. C. P., and Smith, S. J.: Future Arctic temperature change resulting from a range of aerosol emissions scenarios, Earth's Future, 2016.

Wu, Y., Cheng, T., Zheng, L., and Chen, H.: Black carbon radiative forcing at TOA decreased during aging, Scientific reports, 6, 38592, 2016.

Xie, S.-P., Lu, B., and Xiang, B.: Similar spatial patterns of climate responses to aerosol and greenhouse gas changes, Nature Geoscience, 6, 828-832, 2013.

Xu, Y., Lamarque, J.-F., and Sanderson, B. M.: The importance of aerosol scenarios in projections of future heat extremes, Climatic Change, 1-14, 2015.

Yu, S., Alapaty, K., Mathur, R., Pleim, J., Zhang, Y., Nolte, C., Eder, B., Foley, K., and Nagashima, T.: Attribution of the United States "warming hole": Aerosol indirect effect and precipitable water vapor, Scientific reports, 4, 6929, 2014.

Zhao, A., Bollasina, M. A., and Stevenson, D. S.: Strong influence of aerosol reductions on future heatwaves, Geophysical Research Letters, 2019.

Zhao, A. D., Stevenson, D. S., and Bollasina, M. A.: The role of anthropogenic aerosols in future precipitation extremes over the Asian Monsoon Region, Climate Dynamics, 1-22, 2018.

Zheng, B., Tong, D., Li, M., Liu, F., Hong, C., Geng, G., Li, H., Li, X., Peng, L., and Qi, J.: Trends in China's anthropogenic emissions since 2010 as the consequence of clean air actions, Atmospheric Chemistry and Physics, 18, 14095-14111, 2018.

Zhao, A., Stevenson, D. S., and Bollasina, M. A., Climate forcing and response to greenhouse gases, aerosols and ozone in CESM1, Journal of Geophysical Research: Atmosphere, 2019b. in revision.

Table 1 Overview of model experiments. They are: the baseline 1970 (B70) and 2010 (B10) simulation, fixing concentrations of greenhouse gas and ozone in their 1970 levels (SGO), stagnation of anthropogenic aerosol-related emissions from energy use in 1970 levels (SEN), and stagnation of aerosol-related emissions related to technology and abatement measures in 1970 levels (STC). The response to the best estimate of 1970-2010 anthropogenic aerosol-related emissions: best estimate = SGO–

5   B70. Similarly, energy use growth = B10–SEN; technology advances = B10–STC, All simulations are run into equilibrium (numbers in brackets denote the lengths of model integrations in years), and only the last 30 years of each run are used for analysis. Note the difference in the integration lengths, which is determined on the criterion that the top-of-the-atmosphere radiation imbalance no longer shows significant trends (stabilizing at around ~0.3 W m^{-2} in this case) during the last few decades of each run (see the main text).

Experiment (run length, years)	Greenhouse gases	Ozone	Natural aerosols	Anthropogenic aerosols
B70 (120)	1970	1970	1970	1970 best estimate
B10 (150)	2010	2010	2010	2010 best estimate
SGO (90)	1970	1970	1970	2010 best estimate
SEN (220)	2010	2010	2010	2010 STAG_ENE
STC (170)	2010	2010	2010	2010 STAG_TECH
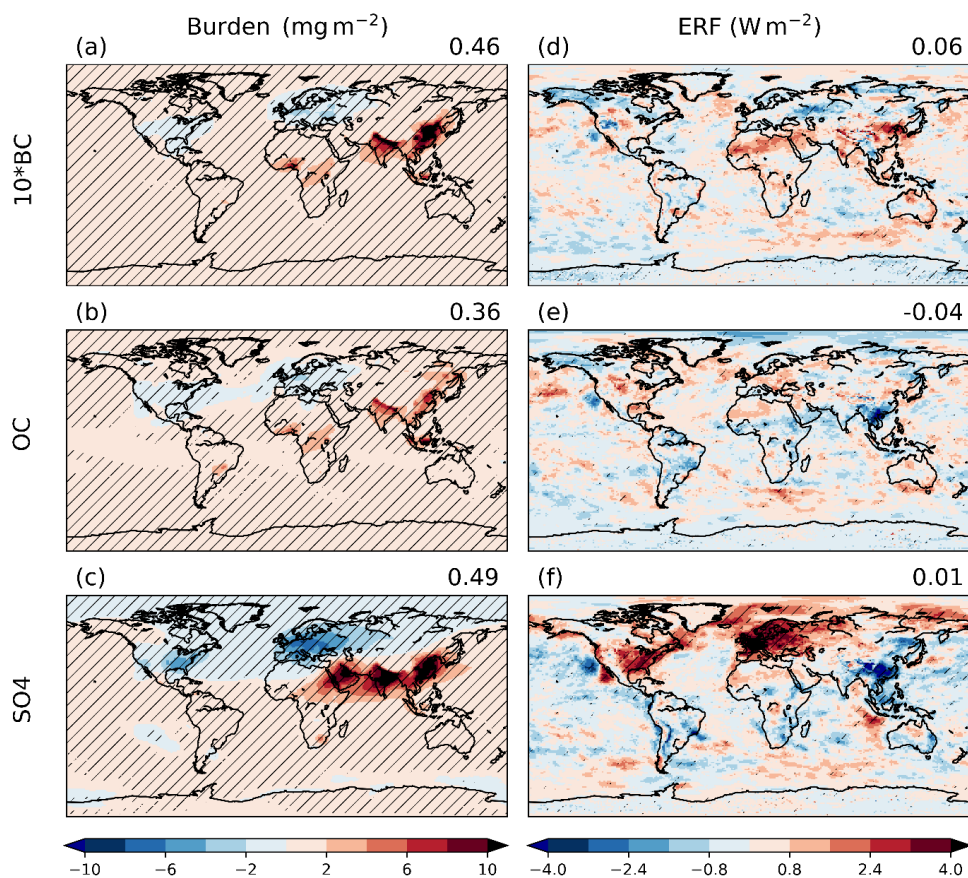
Figure 1 Changes in aerosol burdens (mg m⁻², left) and the effective radiative forcing (ERF, W m⁻², right) associated with the best estimate of 1970-2010 changes in emissions of (**a, d**) black carbon (BC), (**b, e**) organic carbon (OC) and (**e, f**) sulphate species (SO₄). The numbers on the top right of each panel are the global means. NB the burden of BC (including the global mean value) is raised by a factor of 10 for legibility. Hatches, similarly in all other figures, denote 95% statistical significance level derived by a two-tailed student t-test (p-value <0.05).
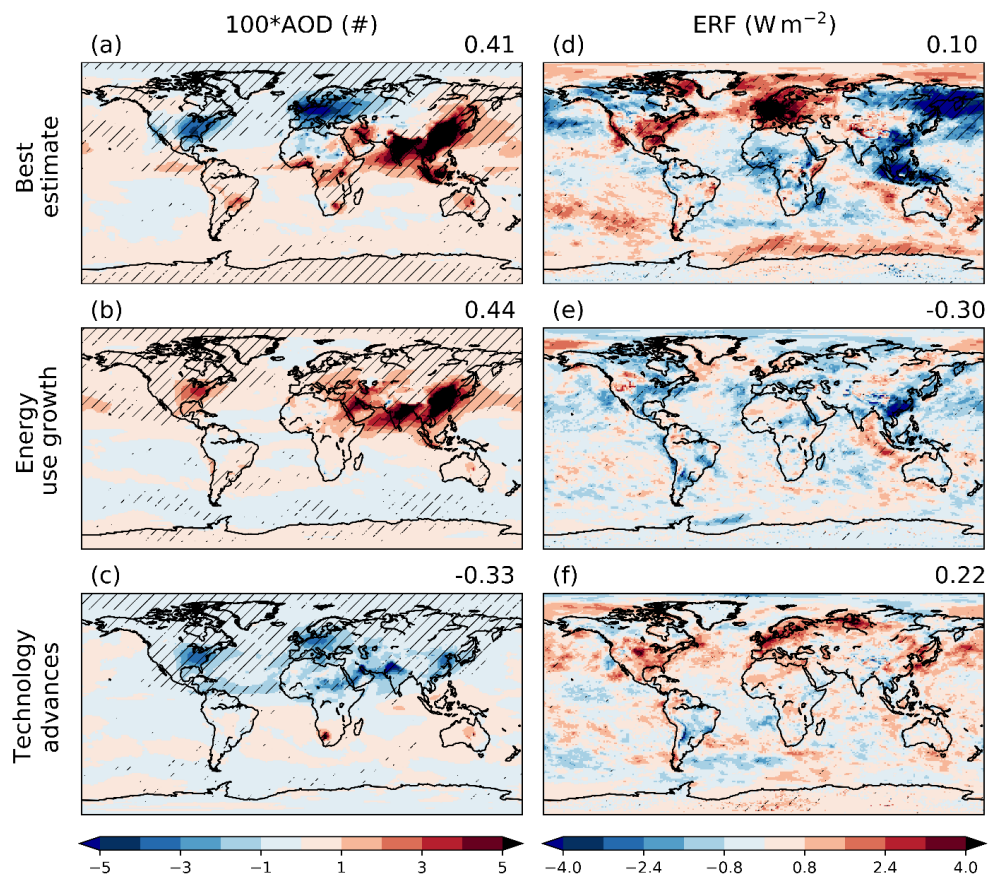
Figure 2. Changes in (**a-c**) 550-nm Aerosol Optical Depth raised up by a factor of 100 (100*AOD) and (**d-f**) the effective radiative forcing (ERF, W m⁻²) in response to 1970-2010 anthropogenic aerosol emissions changes. They are: (**a, d**) the best estimate of total aerosol emission changes, (**b, e**) changes due to energy use growth and (**c, f**) changes due to advances in emission control technology. The numbers on the top right of each panel are the global means (NB again the AOD ones are raised up by a factor of 100).
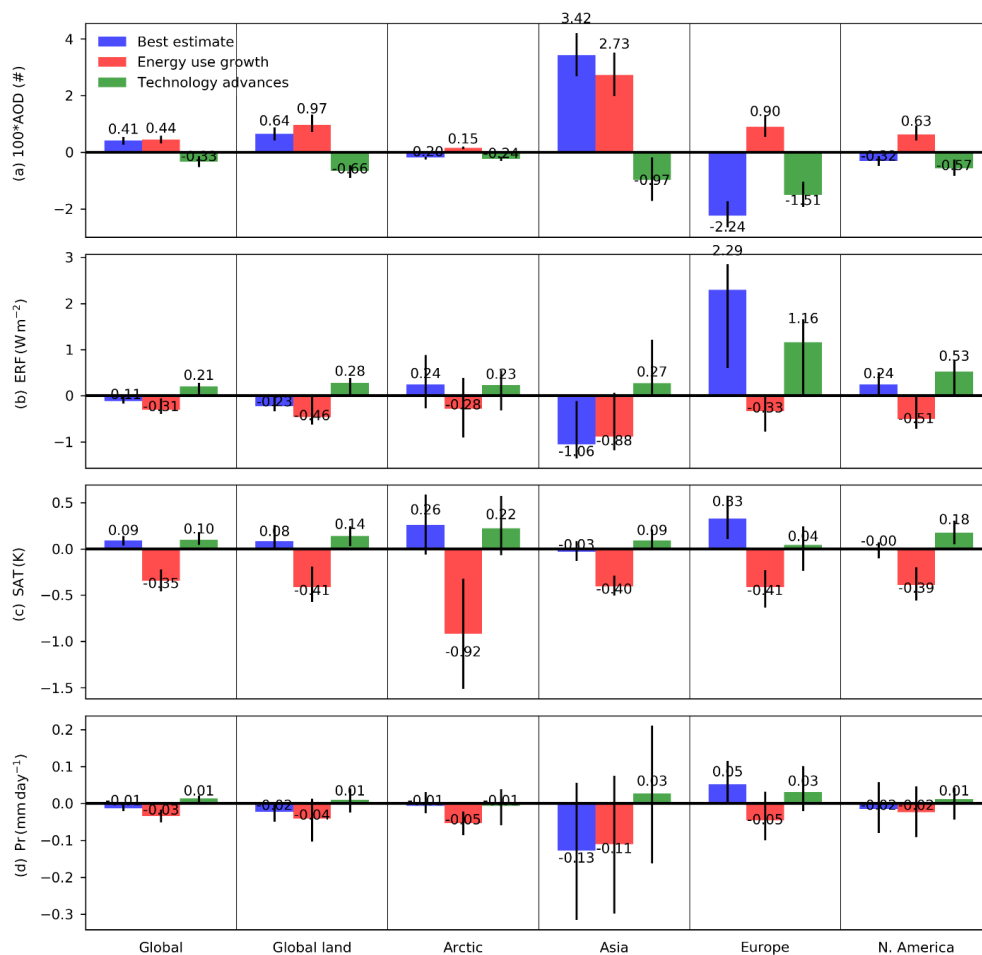
Figure 3. Area-weighted global and regional mean changes in (**a**) Aerosol Optical Depth (100*AOD), effective radiative forcing (ERF, W m^{-2}), surface air temperature (SAT, K), and precipitation (Pr, mm day^{-1}). Error bars denote the 25th–75th percentile spread of the model uncertainty. Region definitions are as follows: Arctic (0°E-360°E, 60°N–0°N), Asia (65°E–145°E, 5°N-45°N), Europe (10°W–40°E, 30°N-70°N) and North America (190°E-300°E, 12°N-70°N). Colour conventions are: blue for responses to the best estimate of 1970-2010 anthropogenic aerosol emissions changes, red for responses to aerosol emission changes due to energy use growth and green for advances in emission control technology. NB carefully that the AOD values are raised up by a factor of 100 for legibility.
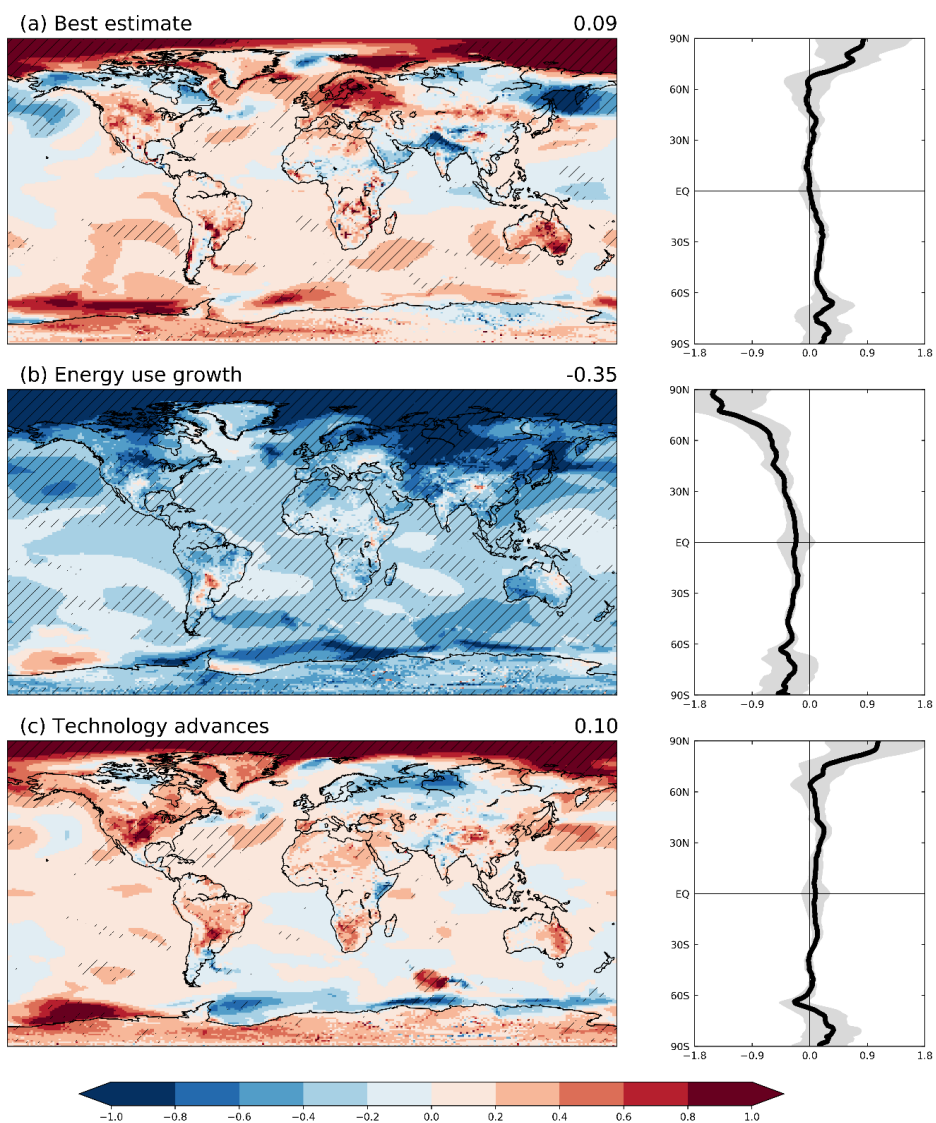
Figure 4 Annual mean surface air temperature change (Δ K), in response to 1970-2010 anthropogenic aerosol emission changes. They are: (**a**) the best estimate of total aerosol emission changes, (**b**) changes due to energy use growth and (**c**) changes due to advances in emission control technology. The numbers on the top right of each panel are the global mean values. Also shown are the mean (solid) and standard deviation (30 model years; shadings) of the zonal mean temperature response.
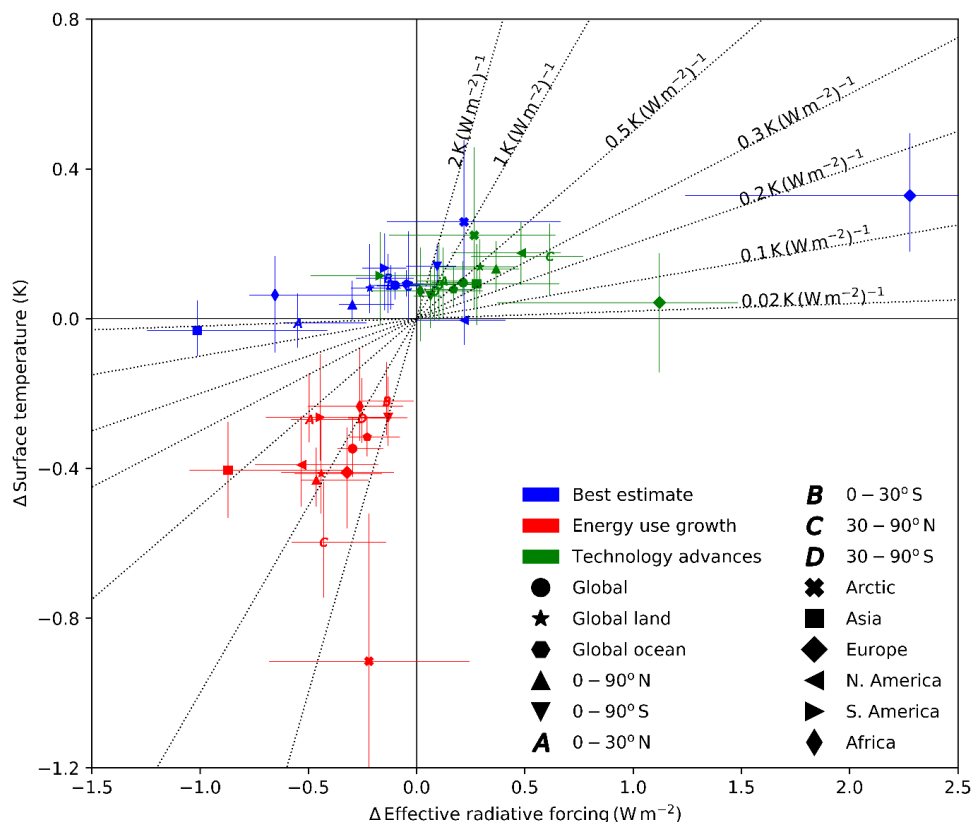
Figure 5. Scatterplot of surface air temperature responses (Δ K) vs. effective radiative forcing (Δ W m^{-2}). The error-bars represent the 25th-75th percentile spread of the model uncertainty. The dashed slope lines crossing the origin indicate the sensitivities of the temperature response to ERF with a unit of K (W m^{-2})$^{-1}$. Region definitions are as follows: Arctic (0°E-360°E, 60°N–0°N), Asia (65°E–145°E, 5°N-45°N), Europe (10°W–40°E, 30°N-70°N), North America (190°E-300°E, 12°N-70°N), South America (278°E-326°E, 56°S-12°N) and Africa (20°W-60°E,-35°S-25°N) plus latitudinal bands. Colour conventions are the same as Fig. 3.
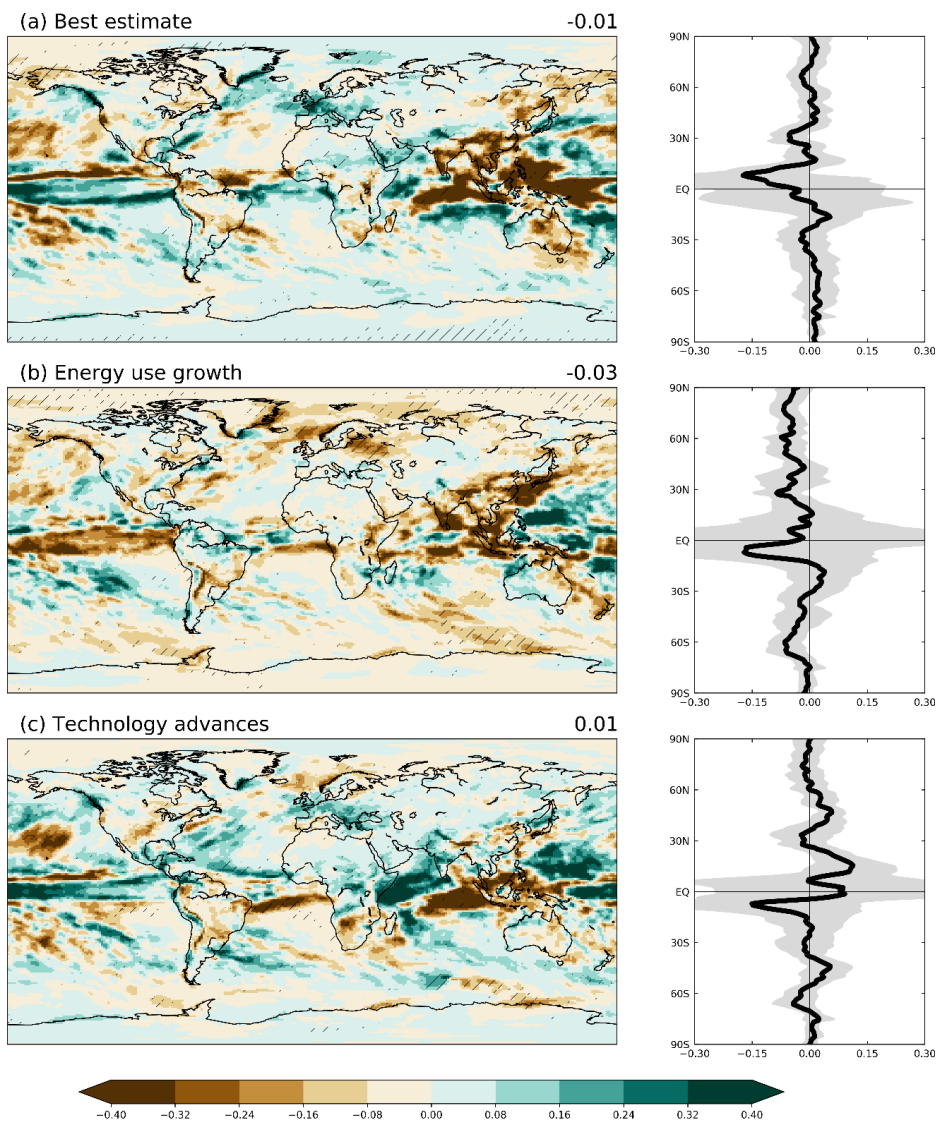
Figure 6 The same as **Fig. 4**, but for precipitation response (Δ mm day⁻¹).